https://doi.org/10.5194/egusphere-2023-175
Preprint. Discussion started: 17 March 2023

Evaluation of TROPOMI operational standard NO_2 column retrievals (from version 1.3 to 2.4) with OMNO2 and QA4ECV OMI observations over China

Jianbin Gu[1,2], Xiaoxia Liang[3], Shipeng Song[4], Yanfang Tian[5], Liangfu Chen[1,2], Jinhua Tao[1,2,*]

[1]State Key Laboratory of Remote Sensing Science, Aerospace Information Research Institute, Chinese Academy of Sciences, Beijing, 100101, China

[2]University of the Chinese Academy of Sciences, Beijing, 100049, China

[3]College of Resource Environment and Tourism, Capital Normal University, Beijing, 100089, China

[4]College of Earth Sciences, Guilin University of Technology, Guilin, 541004, China

[5]State Key Laboratory of Environmental Criteria and Risk Assessment, Chinese Research Academy of Environmental Sciences, Beijing, 100012, China

*Corresponding author: Jinhua Tao

Address: 20 Datun Road, Chaoyang District, State Key Laboratory of Remote Sensing Science, Aerospace Information Research Institute, Chinese Academy of Sciences, Beijing, 100101, China; Tel: +86-10-64889545; Fax: +86-10-64889545; E-mail: 254293974@qq.com

https://doi.org/10.5194/egusphere-2023-175
Preprint. Discussion started: 17 March 2023

Abstract.

The TROPOMI satellite instrument plays a key role in nitrogen dioxide (NO_2) monitoring on account of its unprecedented spatial resolution and stable quality of data. However, since 2019, TROPOMI operational NO_2 retrieval has improved and updated in three versions (1.4, 2.2 and 2.4), with significant impact on retrieved NO_2 column. Thus, studies including both TROPOMI NO_2 data before and after the activation of these versions could show artificial jumps. Moreover, up to date evaluation result of TROPOMI NO_2 data in current version 2.4 is not yet well documented in the literature. Therefore, in this work, we focus on evaluating TROPOMI's capability to detect NO_2 under the different retrieval version conditions, by comparing with OMNO2 data and QA4ECV OMI data over China. We find a 38 % increase of tropospheric NO_2 in version 1.4 due to improved FRESCO-wide cloud retrieval, and a 14 % increase in version 2.2 due to adjusted surface albedo for cloud-free scenes. We show that the upgrade to version 2.4 with new DLER surface albedo, led to an increase by 3 x 10^{14} molecules cm^{-2} of tropospheric NO_2 over vegetation. Furthermore, we demonstrate that TROPOMI data shows strongest tropospheric NO_2 seasonal variation compared to OMNO2 data and QA4ECV OMI data, and this seasonal effect was enhanced with the tropospheric NO_2 retrieval version upgrades. Additionally, we examine for the first time the change of TROPOMI AMFs (air mass factors) in the different versions, and based on it, we arrive at a correction for the underestimation of TROPOMI NO_2 column in previous versions. We also find a 33 % overestimation of NO_2 reduction during the COVID-19 lockdown over China when using TROPOMI data before and after the activation of the NO_2 version 1.4.

Keywords: NO_2, TROPOMI, OMI, QA4ECV, evaluation.

https://doi.org/10.5194/egusphere-2023-175
Preprint. Discussion started: 17 March 2023

1 Introduction

Nitrogen dioxide (NO_2) is an important pollutant trace gas as a primary pollutant and as a precursor to ozone and fine particulate matter production (Cooper et al., 2022). Thus, fast, efficient and accurate monitoring of ambient NO_2 from regional to global scale is indispensable for air quality evaluation and atmosphere pollution control. Among methods of NO_2 monitoring, satellite remote sensing has been widely applied with its large-scale, real-time, simultaneous and high-frequency dynamic monitoring mode. Since 1997, a series of studies on NO_2 monitoring with satellite instruments such as Global Ozone Monitoring Experiment (GOME), Global Ozone Monitoring Experiment-2 (GOME-2), SCanning Imaging Absorption spectro Meter for Atmospheric CHartographY (SCIAMACHY), Ozone Monitoring Instrument (OMI), and TROPOspheric Monitoring Instrument (TROPOMI) has been made, which include monitoring of NO_2 variations (Van der A et al., 2006; Schneider et al., 2015), NO_2 transport phenomena (Nowlan et al., 2014), evaluation of nitrate deposition (Liu et al., 2017b), estimation of nitrogen oxides (NOx = NO + NO_2) emission amounts (Curier et al., 2014; Park et al., 2021) and inference of surface NO_2 concentrations (Gu et al., 2017; Kim et al., 2021).

Among the above-mentioned satellite instruments, the OMI instrument launched in July 2004 is the Dutch-Finnish contribution to National Aeronautics and Space Administration (NASA)'s Earth Observing System (EOS) Aura sensor. It has been used widely to conduct research by applying its long-term observations of NO_2, due to its high spatial resolution and daily global coverage (Levelt et al., 2018; Liu et al., 2017a). As a successor of OMI, since launched in October 2017, the European TROPOMI satellite sensor which is on board the Sentinel-5-Precursor (S5P) has began to play an important role in NO_2 monitoring on account of its unprecedented spatial resolution and stable quality of data (van der A et al., 2020; Ding et al., 2020; Griffin et al., 2019; Zhao et al., 2020). Up to date TROPOMI and OMI are the main data sources in satellite observation of NO_2 (Biswal et al., 2021). Moreover, previous studies focusing on comparative assessment of TROPOMI and OMI NO_2 data have

https://doi.org/10.5194/egusphere-2023-175
Preprint. Discussion started: 17 March 2023

been conducted (Van Geffen et al., 2020; Riess et al., 2022), and the results suggest that data quality of TROPOMI NO_2 observations is significantly improved (Griffin et al., 2019; Wang et al., 2020).

However, currently the following issues should be noted when making study by using TROPOMI NO_2 data. Firstly, TROPOMI NO_2 retrieval algorithm has improved and updated several versions, and three of them (version 1.4, 2.2 and 2.4) have significant impact on retrieved NO_2 column productions. For instance, Riess et al. (2022) found that the improved NO_2 retrieval algorithm in version 1.4 led to increases of TROPOMI NO_2 columns of up to 40 % as compared to version 1.2 in Europe. Thus, studies including both TROPOMI NO_2 data before and after the activation of these versions may show artificial jumps. Secondly, the changes in TROPOMI NO_2 columns caused by these version updates are different, due to their different aspects in improvements of NO_2 retrievals. Additionally, up to date evaluation result of TROPOMI NO_2 data in current version 2.4 (since July 2022) is not yet well documented in the literature. Therefore, in this work, we focus on evaluating TROPOMI's capability to detect NO_2 column in its retrieval version 1.3-2.4 over China, and measuring changes caused by the activation of these versions.

In previous studies NO_2 observations released by ground-based remote sensing techniques such as Pandora and multi-axis differential optical absorption spectroscopy (MAX-DOAS) instruments are generally used to compare and assess NO_2 retrievals derived with satellite instruments (Compernolle et al., 2020; Griffin et al., 2019). However, systematic and consistent ground-based NO_2 observation data has been only provided till November 2017 (e.g. QA4ECV MAX-DOAS data sets, available at http://uv-vis.aeronomie.be/groundbased/QA4ECV_MAXDOAS, last access: 9 October 2022). Thus, in this work, we report a comprehensive evaluation of TROPOMI NO_2 version 1.3-2.4 data products with $OMNO_2$ version 4.0 data products from November 2019 to September 2022 over China. Moreover, the differences between

https://doi.org/10.5194/egusphere-2023-175
Preprint. Discussion started: 17 March 2023

TROPOMI and OMI NO_2 standard data are not only from their instrumental differences, but also from a total uncertainty on their algorithmic differences. Therefore, besides the $OMNO_2$ data, QA4ECV (Quality Assurance for Essential Climate Variables) OMI NO_2 version 1.1 data, which follows a more similar retrieval algorithm as TROPOMI NO_2 data, is also used to compare.

Our study is structured as follows. Sect. 2 provides an introduction to TROPOMI and OMI instrument, as well as their retrievals of NO_2 column, including three main TROPOMI NO_2 retrieval version updates. The information of QA4ECV OMI NO_2 measurement is also given in this section. Sect. 3 presents NO_2 columns, NO_2 spatial-temporal distributions, and seasonal variations over China derived with the TROPOMI data in the different versions (1.3, 1.4, 2.2 and 2.4), by applying the OMNO2 data and QA4ECV OMI NO_2 data as references. The differences between TROPOMI and OMI NO_2 measurements are analysed in relation to their tropospheric NO_2 column discrepancies. Potential causes of the differences (e.g. surface albedo error, cloud parameters and priori profile shape uncertainty) are then discussed. Moreover, AMFs (air mass factors) in the different TROPOMI NO_2 retrieval versions are obtained, and the overestimation of NO_2 reduction during COVID-19 lockdown over China caused by using TROPOMI data before and after the version 1.4 is adjusted. Finally, a conclusion is given in Sect. 4.

2 Description of the data sets

2.1 S5P TROPOMI NO_2

TROPOMI is a nadir-viewing spectrometer aboard European Space Agency (ESA)'s the S5P satellite (Van Geffen et al., 2020). It is designed to monitoring atmospheric components including ozone (O_3), NO_2, sulfur

https://doi.org/10.5194/egusphere-2023-175
Preprint. Discussion started: 17 March 2023

dioxide (SO_2), carbon monoxide (CO) and formaldehyde (HCHO) with daily global coverage, as the successor of OMI (Veefkind et al., 2012). TROPOMI traces a sun-synchronous polar orbit with an equator crossing at about 13:30 local time, and provides observation data in four channels covering ultraviolet (UV) to shortwave infrared wavelengths. In the visible (VIS) channel (400 nm-496 nm) used for NO_2 retrieval, TROPOMI's horizontal resolution at true nadir is improved to an unprecedented extent than the previous satellite instruments (De Smedt et al., 2018). Its observation individual pixels are 7 km (5.5 km since August 2019) as an integration time of 1.08 s in the along-track, and 3.5 km in the across-track direction at the middle of the swath. Along the across-track direction there are 450 ground pixels in a row, and these pixel sizes remain more or less constant towards the edges of the swath (the largest pixels are 14 km wide) (Van Geffen et al., 2020).

The TROPOMI NO_2 retrieval which is developed by the Royal Netherlands Meteorological Institute (KNMI) (Van Geffen et al., 2020) consists of a three-step procedure: (1) Deriving of a total atmospheric NO_2 slant column density (SCD) using the Differential Optical Absorption Spectroscopy (DOAS) retrieval method in the 405 nm-465 nm spectral range. (2) Separation of the retrieval total NO_2 SCD into a stratospheric NO_2 SCD and a tropospheric NO_2 SCD based on the TM5-MP model (Williams et al., 2017). (3) Normalization of a tropospheric NO_2 vertical column density (VCD) from the retrieval tropospheric NO_2 SCD by applying an appropriate AMF. The AMF is defined as the ratio of the observed SCD of the absorbing trace gas along the slant optical path from sun to satellite, and the vertical column density above the point at the surface area the satellite is viewing. More details of the TROPOMI NO_2 retrieval are described in the product Algorithm Theoretical Basis Document (Van Geffen et al., 2020).

https://doi.org/10.5194/egusphere-2023-175
Preprint. Discussion started: 17 March 2023

2.1.1 Improved FRESCO-wide cloud retrievals in version 1.4

Tropospheric AMF uncertainty is the largest source of satellite-derived tropospheric NO_2 column uncertainty for polluted scenes, ranges between 20 %-50 %, leading to a total uncertainty in tropospheric NO_2 column in the 30 %-60 % range (Liu et al., 2021). The NO_2 AMF to harmonize the conversion of SCD into VCD is calculated using the Doubling-Adding KNMI (DAK) radiative transfer model (Lorente et al., 2017), and the input parameters to the TROPOMI NO_2 AMF calculation are surface albedo climatology (Kleipool et al., 2008), priori NO_2 profiles (Williams et al., 2017), viewing geometry (satellite and solar angles), terrain height and cloud parameters (Riess et al., 2022), including cloud pressure retrieved with the TROPOMI FRESCO cloud algorithm (driven by the 761 and 765 nm O_2 absorption depth). With the introduction of version 1.4 in December 2020, a new FRESCO-wide cloud algorithm was introduced and implemented in the TROPOMI operational NO_2 retrieval to address the high-bias in the previous FRESCO cloud pressures used in version 1.0-1.3. The main improvement by the FRESCO-wide algorithm is an overall reduction of the observed cloud pressures, resulting in a decrease of AMFs and a substantial increase of NO_2 in the retrievals in polluted regions.

2.1.2 Adjusted surface albedo in version 2.2-2.3

From July 2021 onwards, for TROPOMI NO_2 version 2.2, a surface albedo adjustment was implemented to avoid negative cloud fractions while maintaining radiance closure. For instance, cloud fraction varies between 0 and 1 on physical grounds, and when the actual surface albedo is lower than expected from the Kleipool et al. (2008) surface albedo climatology, it leads to a negative cloud fraction. In the previous TROPOMI NO_2 version retrievals, this was clipped to 0. But with the implementation of version 2.2, surface albedo is decreased to match cloud fraction equal 0, and thus, ensure radiance closure (Van Geffen et al., 2022). Additionally, the Kleipool et al. (2008) surface albedo climatology based on OMI data does not cover the near-infrared wavelengths in use by

https://doi.org/10.5194/egusphere-2023-175
Preprint. Discussion started: 17 March 2023

the FRESCO algorithm to derive cloud properties, and, instead, up to version 2.3 the surface albedo database used by the FRESCO algorithm is based on GOME-2 observations (Tilstra et al., 2017) at 758 and 772 nm. The overpass time of GOME-2 is several hours earlier relative to OMI and TROPOMI, which is in favour of the Kleipool surface albedo climatology for the NO_2 retrieval, and to determine the cloud fraction in the NO_2 window (S5P-KNMI-L2-0005-RP, available at https://sentinel.esa.int/documents/247904/2476257/Sentinel-5P-TROPOMI-ATBD-NO2-data-products; last access: 9 October 2022). As a consequent, these lead to a significant increase (10 %-15 %) of TROPOMI tropospheric NO_2 for cloud-free scenes on top of the increase for pixels with small cloud fractions in version 1.4 related to the improved FRESCO-wide cloud retrievals.

We note that the NO_2 fit window of the wavelength was not correct in TROPOMI version 2.2, with negligible effect on the NO_2 column retrieval, while it was corrected in version 2.3 (405 nm-465 nm). Thus, TROPOMI NO_2 version 2.3 product is the most complete and consistent to date. Zhang et al. (2023) report on the improvement of TROPOMI version 2.3 NO_2 columns, and their impact on emission estimates specifically over China in times of COVID-19 lockdowns. Additionally, to consistent with the extents of improvements for version 2.2 and 2.3 released by the ESA S5P/TROPOMI NO_2 algorithm change record (S5P-MPC-KNMI-PRF-NO2, available at http://sentinels.copernicus.eu/web/sentinel/technical-guides/sentinel-5p/products-algorithms/; last access: 9 October 2022), in this work TROPOMI version 2.2 and 2.3 NO_2 column products are collectively referred to as the former.

2.1.3 Alternative surface albedo climatology in version 2.4

With the introducing of TROPOMI NO_2 version 2.4 in July 2022, a Directional Lambertian Equivalent Reflectivity (DLER) climatology derived from TROPOMI observations replaced the original surface albedo

https://doi.org/10.5194/egusphere-2023-175
Preprint. Discussion started: 17 March 2023

climatologies derived from OMI and GOME-2 in older versions 1.0-2.2. This new DLER climatology is applied in cloud fraction and cloud pressure retrievals in the NO_2 window, using in the TROPOMI NO_2 AMF calculation. It has several advantages in the represent of the directionality or viewing-angle dependence of the scattering at the surface, as well as the improved spatial resolution of the surface albedo climatology database from 0.5 x 0.5 degree to 0.125 x 0.125 degree. But up to date the impact of the DLER climatology in version 2.4 to the TROPOMI NO_2 column retrieval has not yet been released.

2.2 Aura OMI NO_2

The OMI sensor launched in July 2004 was installed on NASA's Earth Observing System Aura satellite. It is designed to continue the Total Ozone Mapping Spectrometer (TOMS) record for O_3 and other atmospheric component products such as NO_2, SO_2 and HCHO (Boersma et al., 2007). OMI is a nadir-viewing imaging spectrograph that measures direct and atmosphere-backscattered sunlight within an UV - VIS range of 270 nm-500 nm (Levelt et al., 2006). It traces a sun-synchronous ascending polar orbit with an equator crossing time of 13:30. The spatial resolution of OMI NO_2 product is about 13 x 24 km^2 at nadir. Along the cross track, OMI pixel sizes vary with viewing zenith angles from 24 km in the nadir to approximately 128 km in extreme viewing angles of 57 degree along the edges of the swath (Boersma et al., 2007). Since October 2004 OMI has provided various trace gas concentration observations with daily global coverage. It should be noted that after May 2008 with the introduction of the row anomaly, OMI no longer provides daily global coverage.

The OMI NO_2 (OMNO2) retrieval algorithm consists of a three-step procedure. (1) a spectral fitting algorithm to calculate total NO_2 SCD in the 402 nm-465 nm spectral range. (2) a stratosphere-troposphere separation scheme

https://doi.org/10.5194/egusphere-2023-175
Preprint. Discussion started: 17 March 2023

to derive tropospheric and stratospheric NO_2 VCDs. (3) determination of AMF to convert SCD to VCD. Detailed descriptions of the OMNO2 retrieval algorithm were provided by Bucsela et al. (2013) and Celarier et al. (2008).

Up to date a series of significant conceptual and technical improvements in the OMNO2 retrieval has been made. A new scheme for seperating stratospheric and tropospheric components was implemented in the OMNO2 version 2.1 (Lamsal et al., 2014). With the introduction of version 3.0, a significant advance of NO_2 SCD retrieval was developed (Krotkov et al., 2017). The current version, 4.0, a several changes for improved NO_2 AMF and VCD calculations are introduced, including applying a new geometry dependent surface Lambertian Equivalent Reflectivity product in NO_2 retrieval (Fasnacht et al., 2019), as well as improved cloud parameter retrievals (effective cloud fraction and optical centroid pressure from a new cloud OMCDO2N algorithm) (Vasilkov et al., 2018).

2.3 QA4ECV OMI NO_2

The EU Seventh Framework Programme QA4ECV project (http://www.qa4ecv.eu, last access: 9 October 2022) was initiated in 2014. It aims to demonstrated how reliable and traceable quality information can be provided for satellite and ground-based measurements of climate and air quality parameters (Compernolle et al., 2020). The project developed and applied a quality assurance framework on new and improved satellite data records of the atmosphere ECVs including NO_2, HCHO and CO.

The QA4ECV OMI NO_2 version 1.1 product is retrieved from OMI Level 1 UV-Vis spectral measurements, and its retrieval algorithm is based on the DOAS approach, like the OMNO2 product (Boersma et al., 2018). The differences between OMNO2 and QA4ECV OMI NO_2 product account for estimating the stratospheric SCD and

https://doi.org/10.5194/egusphere-2023-175
Preprint. Discussion started: 17 March 2023

calculating the tropospheric AMF (e.g. the prior NO_2 profiles information and the cloud retrieval). Previous evaluations suggest that the discrepancies between OMNO2 and QA4ECV OMI tropospheric NO_2 VCD retrievals typically lead to small but spatially widespread differences of up to 0.5-1 x 10^{15} molecules cm^{-2} (Compernolle et al., 2020). On the other hand, the retrieval of tropospheric NO_2 from QA4ECV OMI proceeds along the same lines as from TROPOMI, and is thus similar in many aspects (Riess et al., 2022).

2.4 Screening criteria

The details on the retrievals of the TROPOMI, OMNO2 and QA4ECV OMI tropospheric NO_2 column are given, see Table 1. In this work we compared the TROPOMI tropospheric NO_2 version 1.3-2.4 data to the OMNO2 tropospheric NO_2 version 4.0 data and QA4ECV OMI tropospheric NO_2 version 1.1 data in order to evaluate their capabilities to detect NO_2. We selected these satellite data for tropospheric NO_2 column evaluation if the following conditions are met:

(1) TROPOMI NO_2 column products taken a sufficient quality of retrieval (qa_value > 0.50);

(2) $OMNO_2$ column products where the XtrackQualityFlags field is equal to 0, for selecting only rows which have not been affected by the row anomaly;

(3) QA4ECV OMI NO_2 column products where the processing_error_flag field is equal to 0;

(4) All satellite NO_2 column products taken an effective cloud fraction less than 0.2;

(5) All satellite NO_2 column products taken a satellite solar zenith angle less than 80 degree.

Table 1. Retrievals for the TROPOMI version 1.3-2.4, OMNO2 version 4.0 and QA4ECV OMI version 1.1 tropospheric NO_2 column used in this study.

	TROPOMI	TROPOMI	TROPOMI	TROPOMI	OMNO2	QA4ECV

https://doi.org/10.5194/egusphere-2023-175
Preprint. Discussion started: 17 March 2023

	v1.3	v1.4	v2.2	v2.4	v4.0	OMI v1.1
Public data period	20 Mar 2019-29 Nov 2020	29 Nov 2020-01 Jul 2021	01 Jul 2021-17 Jul 2022	17 Jul 2022-	01 Oct 2004-	01 Oct 2004-30 Mar 2021
Spectral fitting	Van Geffen et al. (2020)	Van Geffen et al. (2020)	Van Geffen et al. (2020)	Van Geffen et al. (2020)	Marchenko et al. (2015)	Zara et al. (2018)
Surface albedo	Kleipool et al. (2008) 5-year climatology at 0.5° x 0.5°	Kleipool et al. (2008) 5-year climatology at 0.5° x 0.5°	Kleipool et al. (2008) 5-year climatology at 0.5° x 0.5° (adjusted)	TROPOMI DLER climatology at 0.125° x 0.125°	Kleipool et al. (2008) 5-year climatology at 0.5° x 0.5°	Kleipool et al. (2008) 5-year climatology at 0.5° x 0.5°
A priori NO_2 profiles	Daily TM5-MP at 1° x 1°	Daily TM5-MP at 1° x 1°	Daily TM5-MP at 1° x 1°	Daily TM5-MP at 1° x 1°	Monthly Global Modelling Initiative data at 1° x 1.25°	Daily TM5-MP at 1° x 1°
Clouds retrieval	FRESCO	FRESCO-wide	FRESCO-wide	FRESCO-wide	OMCDO2N	OMCLDO2
Stratospheric correction	Data assimilation in TM5-MP	Data assimilation in TM5-MP	Data assimilation in TM5-MP	Data assimilation in TM5-MP	Bucsela et al. (2013)	Data assimilation in TM5-MP

https://doi.org/10.5194/egusphere-2023-175
Preprint. Discussion started: 17 March 2023

236

237 3 Results and discussion

238 3.1 NO_2 columns and trends

239 We start with evaluating TROPOMI's capability to detect tropospheric NO_2 with the OMNO2 and QA4ECV
240 OMI NO_2 observations. First, we create 7 x 7 km^2 TROPOMI tropospheric NO_2 VCD version 1.3-2.4 daily data
241 and 0.25 x 0.25 degree OMNO2 tropospheric VCD version 4.0 daily data from November 2019 to September
242 2022, as well as QA4ECV OMI tropospheric NO_2 VCD version 1.1 daily data from November 2019 to March
243 2021, as described in Section 2.4. Then, we derive the daily means of these data sets over China which have not
244 been selected for co-sampling, in order to ensure their respective data validity, and the monthly means of relative
245 differences between them are further calculated (Fig. 1). Meteorological effects were generally minor at the
246 national scale.

247

https://doi.org/10.5194/egusphere-2023-175
Preprint. Discussion started: 17 March 2023

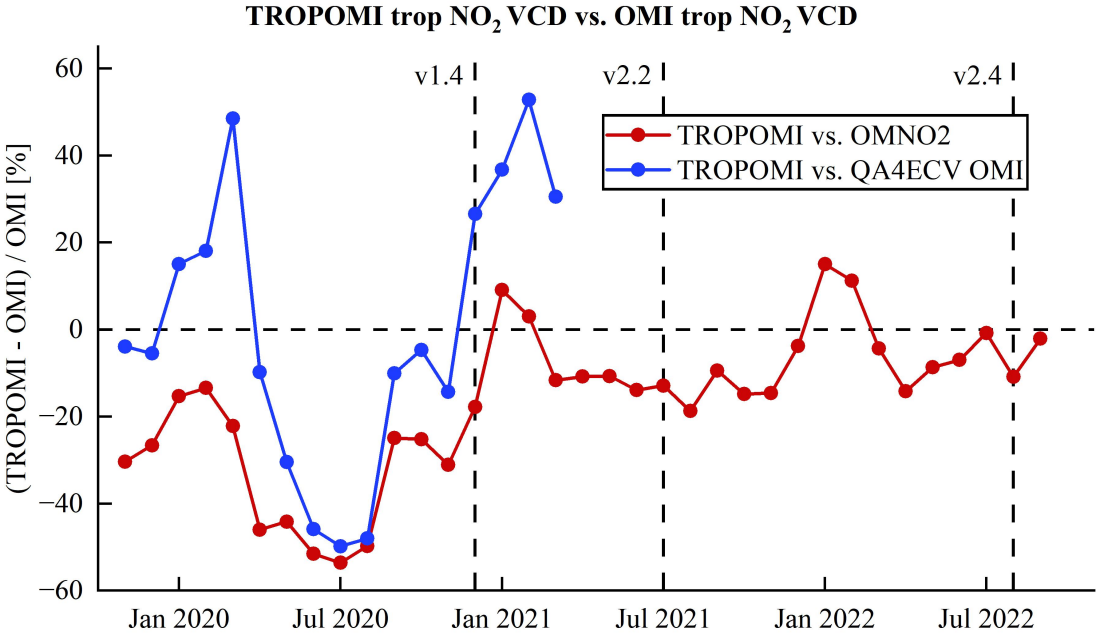

Figure 1. Relative differences between TROPOMI (version 1.3-2.4) and OMNO2 tropospheric NO_2 VCDs from November 2019 to September 2022 (red), and between TROPOMI and QA4ECV OMI tropospheric NO_2 VCDs from November 2019 to March 2021 (blue) over the whole China. The black vertical line represents the date when the TROPOMI NO_2 retrieval version started.

The tropospheric NO_2 VCDs over China derived from TROPOMI version 1.3 observations are overall lower by 33 ± 14 % and 11 ± 28 % than those derived from OMNO2 and QA4ECV OMI observations respectively (Fig. 1). This can be explained by the overestimation of the FRESCO cloud pressures, and subsequently the overestimation of the AMFs, and thus, the underestimation of the tropospheric NO_2 columns for scenes with small cloud fractions in the TROPOMI NO_2 version 1.3. Moreover, the TROPOMI tropospheric NO_2 VCDs have the largest decrease in the summer months (e.g. 52 % for June, 54 % for July and 50 % for August), and the smallest decrease in the winter months (e.g. 15 % for January, 13 % for February and 22 % for March), as

https://doi.org/10.5194/egusphere-2023-175
Preprint. Discussion started: 17 March 2023

compared to the OMNO2 tropospheric VCDs. Similar seasonal differences exist in the comparison of the TROPOMI tropospheric NO_2 VCDs to the QA4ECV OMI tropospheric NO_2 VCDs (e.g. −46 % for June, −50 % for July, − 48 % for August and 15 % for January, 18 % for February, 49 % for March). These seasonal differences in decrease of the TROPOMI tropospheric NO_2 version 1.3 columns relative to the tropospheric NO_2 columns derived from OMI exhibit a summer maximum and winter minimum, in contrast to the winter maximum and summer minimum in TROPOMI or OMI total NO_2 columns.

We also compare the TROPOMI tropospheric NO_2 VCD daily data from December 2020 to June 2021 (the entire version 1.4 period), to the OMNO2 and QA4ECV OMI tropospheric NO_2 VCD daily data over China. We find that the extent of the decrease between the TROPOMI and OMNO2 tropospheric NO_2 VCDs has become smaller between December 2020 and June 2021 ($1.89 \pm 3.08 \times 10^{14}$ molecules cm^{-2}) than between December 2019 and June 2020 ($6.59 \pm 3.18 \times 10^{14}$ molecules cm^{-2}). Similarly, the extent of the increase between TROPOMI and QA4ECV OMI tropospheric NO_2 VCDs has become larger between December 2020 and March 2021 ($6.99 \pm 1.74 \times 10^{14}$ molecules cm^{-2}) than between December 2019 and March 2020 ($2.13 \pm 2.92 \times 10^{14}$ molecules cm^{-2}). Therefore, we conclude that the upgrade to version 1.4 with the improved FRESCO-wide cloud retrieval, led to a significant increase (about 5×10^{14} molecules cm^{-2}) of tropospheric NO_2 columns as compared with the previous version. As a consequence, the low bias in the TROPOMI tropospheric NO_2 columns prior to November 2020 was (at least partly) addressed.

An increase (22 %-35 %) in the TROPOMI tropospheric NO_2 version 1.4 columns over China is measured by comparing with the QA4ECV OMI tropospheric NO_2 columns between December 2020 to March 2021 than between December 2019 to March 2020 (Fig. 2). Similar increase (19 %-32 %) was observed by comparing the TROPOMI version 1.4 tropospheric NO_2 VCDs to the OMNO2 tropospheric VCDs during the same periods. We

https://doi.org/10.5194/egusphere-2023-175
Preprint. Discussion started: 17 March 2023

284 conclude that the TROPOMI NO_2 column enhancement (of up to 38 %) was identified from version 1.3 to 1.4
285 over China, due to the improved cloud information retrievals. This conclusion is in agreement with previous
286 validation studies by Riess et al. (2022) who found that the improved cloud pressures in version 1.4 led to
287 increases of TROPOMI NO_2 columns of up to 40 % in Europe, and by (S5P-MPC-KNMI-PRF-NO2) who found
288 an increase of up to 50 % in TROPOMI NO_2 version 1.4 over East Asia.
289

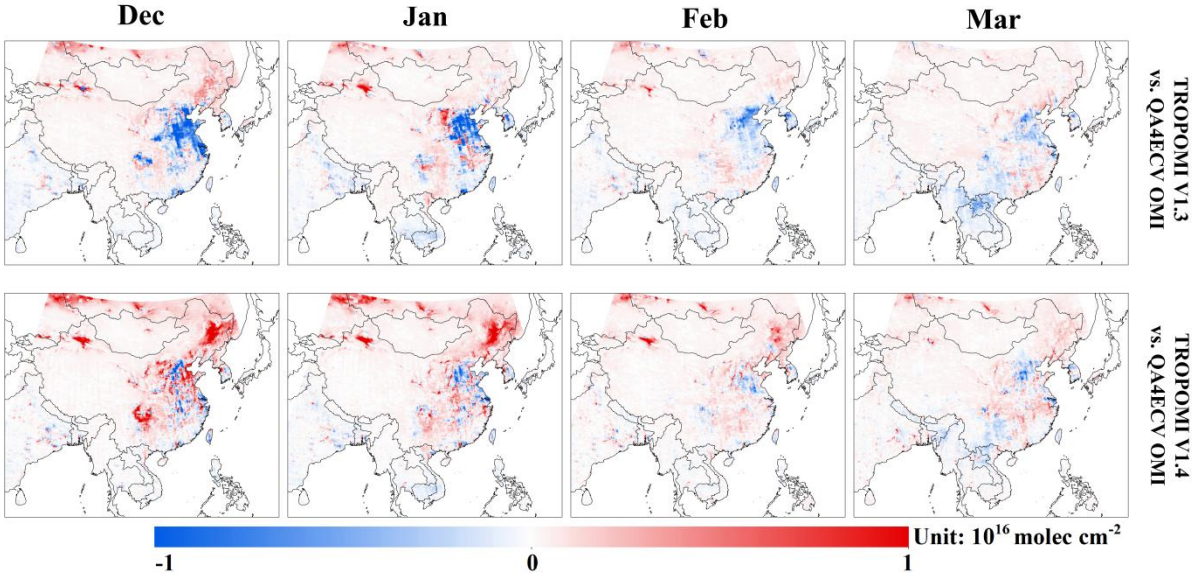

290

291 **Figure 2.** Differences in monthly mean tropospheric NO_2 columns derived from TROPOMI data and QA4ECV
292 OMI data (TROPOMI minus QA4ECV) between December 2019 and March 2020 (first row, TROPOMI version
293 1.3), and between December 2020 and March 2021 (second row, TROPOMI version 1.4). NO_2 columns derived
294 using TROPOMI observations gridded at 0.25 x 0.25 degree resolution.
295

296 Since the QA4ECV OMI NO_2 data product is available before 30 March 2021, here, we compare the TROPOMI
297 NO_2 columns only to the $OMNO_2$ columns after the date. Throughout the entire version 2.2 period (from July

https://doi.org/10.5194/egusphere-2023-175
Preprint. Discussion started: 17 March 2023

2021 to June 2022), the TROPOMI tropospheric NO_2 VCDs are lower by 1.30 ± 2.52 x 10^{14} molecules cm^{-2} compared to the OMNO2 tropospheric VCDs over China. Furthermore, this decrease is weakest in the winter of 2021/2022 (-1.84 x 10^{14} molecules cm^{-2}) and strongest in the summer of 2021 (2.57 x 10^{14} molecules cm^{-2}). This seasonal trend of the difference between the TROPOMI tropospheric version 2.2 NO_2 and the $OMNO_2$ is similar with that between the TROPOMI tropospheric version 1.4 NO_2 and the $OMNO_2$. It can be explained by the surface albedo adjusted to avoid negative cloud fractions while maintaining radiance closure in TROPOMI NO_2 version 2.2, and thus, this adjust can lead to a significant increase of tropospheric NO_2 columns for cloud-free scenes which occur frequently in winter and rarely in summer in China. Additionally, an increase of up to 14 % in the TROPOMI tropospheric NO_2 columns in version 2.2 is measured by comparing with the OMNO2 tropospheric columns between December 2021 to March 2022 compared to the previous year.

We compare the TROPOMI tropospheric NO_2 version 2.4 daily VCDs retrieved with the new DLER surface albedo climatology used in the FRESCO-wide cloud fraction and cloud pressure retrievals, to the OMNO2 tropospheric daily VCDs from August to September 2022. As a result, the extent of the difference between the TROPOMI and OMNO2 tropospheric VCDs has decreased between August and September 2022 (1.04 x 10^{14} molecules cm^{-2}) compared to the previous year (2.31 x 10^{14} molecules cm^{-2}) over China. We find that the DLER surface albedo climatology in tropospheric AMF calculating in version 2.4 led to a 6 % increase of TROPOMI tropospheric NO_2 columns over China. This is consistent with previous validation study by (S5P-MPC-KNMI-PRF-NO2) who suggest that the impact of the DLER surface albedo climatology in TROPOMI NO_2 version 2.4 retrievals over Europe, North America and East China is relatively minor.

Overall, tropospheric NO_2 columns derived from TROPOMI, OMNO2 and QA4ECV OMI provide a similar initial baseline over China (Fig. 3). They exhibit a clear spatial pattern of tropospheric NO_2 with the higher

https://doi.org/10.5194/egusphere-2023-175
Preprint. Discussion started: 17 March 2023

pollution levels over the Beijing-Tianjin-Hebei (BTH), Yangtze River Delta (YRD) and Pearl River Delta (PRD) region, due to the combined effects of local developed industrialization and huge population density. On the other hand, in general, compared to OMNO2, QA4ECV OMI NO_2 follows a more similar retrieval algorithm as TROPOMI NO_2, thus comparison between TROPOMI NO_2 and QA4ECV OMI NO_2 is much more direct as the algorithmic differences between them will cancel, exposing better the main instrumental differences. Consequently, the difference between TROPOMI version 1.3 NO_2 VCD and OMNO2 VCD (7.18 x 10^{14} molecules cm^{-2}, 47 %) is considerably larger than that between TROPOMI version 1.3 NO_2 VCD and QA4ECV OMI NO_2 VCD (1.97 x 10^{14} molecules cm^{-2}, 13 %). Additionally, the annual average tropospheric NO_2 VCD over China derived from TROPOMI version 1.3, OMNO2 and QA4ECV OMI is 1.52 ± 0.63 x 10^{15}, 2.24 ± 0.72 x 10^{15} and 1.71 ± 0.55 x 10^{15} molecules cm^{-2} respectively. Compared to the OMNO2 tropospheric VCDs, the lower QA4ECV OMI tropospheric NO_2 VCDs are most likely interpreted with their differences between the tropospheric AMF calculations (and especially the priori NO_2 profiles information, see Table 1) (Goldberg et al., 2017).

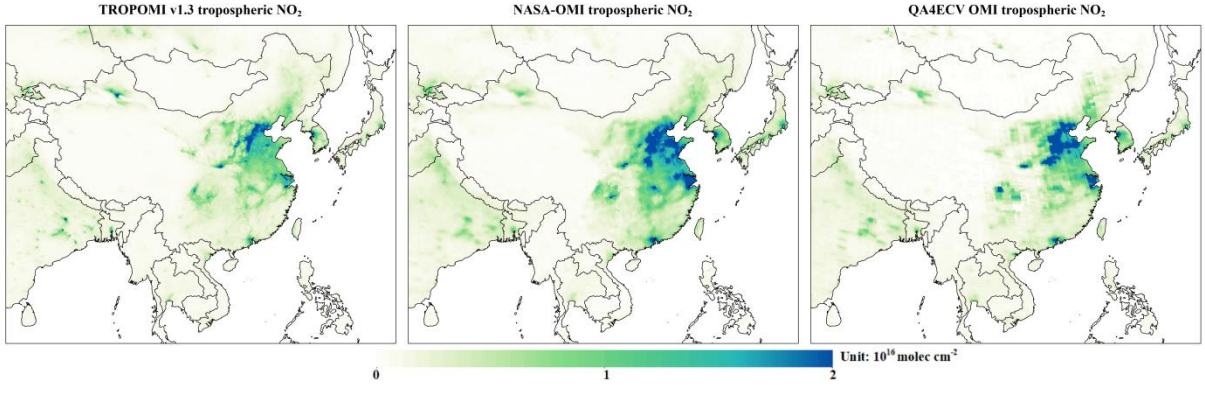

Figure 3. November mean tropospheric NO_2 columns derived from TROPOMI version 1.3 (left panel), OMNO2 (center panel) and QA4ECV OMI (right panel) observations in 2019.

https://doi.org/10.5194/egusphere-2023-175
Preprint. Discussion started: 17 March 2023

3.2 TROPOMI NO_2 version 2.4 over vegetation

The impact of the upgrade to version 2.4 on TROPOMI NO_2 column at national scale are given in Section 3.1. However, the DLER surface albedo using in TROPOMI version 2.4 accounts for the directionality or viewing-angle dependence of the scattering at the surface, especially over vegetation in the near infrared. Thus according to this strong effect of the DLER over vegetation, we evaluate to the new DLER surface albedo in and its impact on the TROPOMI NO_2 columns, to better understand the recent detection of NO_2 under condition of vegetation coverage. In this section, we compare the TROPOMI tropospheric NO_2 VCD daily data in August of 2020 (version 1.3), 2021 (version 2.2) and 2022 (version 2.4) over Fujian Province (the province with the highest vegetation coverage in China), as well as over China as a reference (Fig. 4).

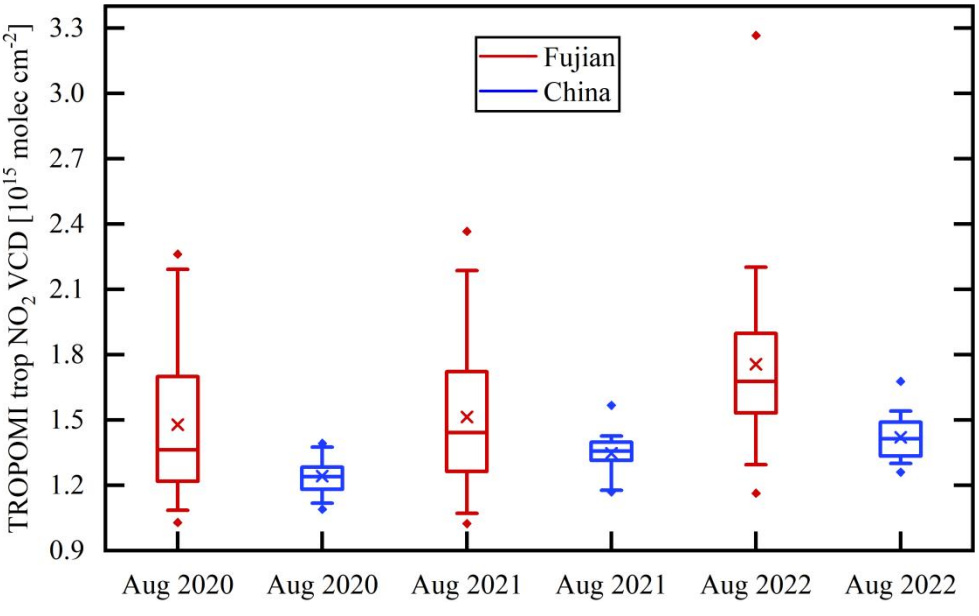

Figure 4. Boxplots of daily TROPOMI tropospheric NO_2 columns in August of 2020 (version 1.3), 2021 (version 2.2) and 2022 (version 2.4) over Fujian Province (red), and over China (blue). The box edges represent

https://doi.org/10.5194/egusphere-2023-175
Preprint. Discussion started: 17 March 2023

the 1st and 3th quartiles, the line in the box represents the median, the cross in the box represents the mean, the dots represent the outlier, and the whiskers represent the 5th and 95th percentiles.

We find that from version 1.3 to 2.2 to 2.4, the TROPOMI tropospheric NO_2 column over China is increased by 9 % (1.06 x 10^{14} molecules cm^{-2}) and 5 % (0.73 x 10^{14} molecules cm^{-2}) respectively, and in comparison, the increase in TROPOMI tropospheric NO_2 column over Fujian from version 1.3 to 2.2 is relatively minor (2 %, 0.35 x 10^{14} molecules cm^{-2}), but the tropospheric NO_2 enhancements over this region from version 2.2 to 2.4 are presented, with a substantial increase (16 %, 2.42 x 10^{14} molecules cm^{-2}). We also compare the TROPOMI tropospheric NO_2 daily VCDs to the OMNO2 tropospheric daily VCDs between August to September in 2021 and 2022 over Fujian. As a result, the upgrade to version 2.4 with the DLER surface albedo, led to a significant increase (about 3.44 x 10^{14} molecules cm^{-2}) of tropospheric NO_2 columns as compared with the previous version over vegetation.

3.3 NO_2 seasonal cycle

NO_2 has obvious seasonal variation characteristics with low in summer and high in winter, as NO_2 lifetime could prolong due to low solar irradiances and low specific humidity (Bauwens et al., 2020). Previous studies suggest that TROPOMI and OMI can effectively reflect the NO_2 seasonal variation on account of their high temporal and spatial resolutions (Dimitropoulou et al., 2020; Meng et al., 2018). Here, we use TROPOMI (version 1.3-2.2), OMNO2 and QA4ECV OMI NO_2 observations from November 2019 to June 2022 to explore their sensitivities to the NO_2 seasonal variation. We select three periods based on the TROPOMI NO_2 retrieval version updates as follows: December 2019 to November 2020 (version 1.3), December 2020 to June 2021 (version 1.4) and July 2021 to June 2022 (version 2.2). Then, we calculate the ratios of the January and June mean tropospheric NO_2

https://doi.org/10.5194/egusphere-2023-175
Preprint. Discussion started: 17 March 2023

VCD in each period to the averaged tropospheric NO_2 VCD over the entire period over China retrieved from TROPOMI, OMNO2 and QA4ECV OMI observations respectively (Fig. 5).

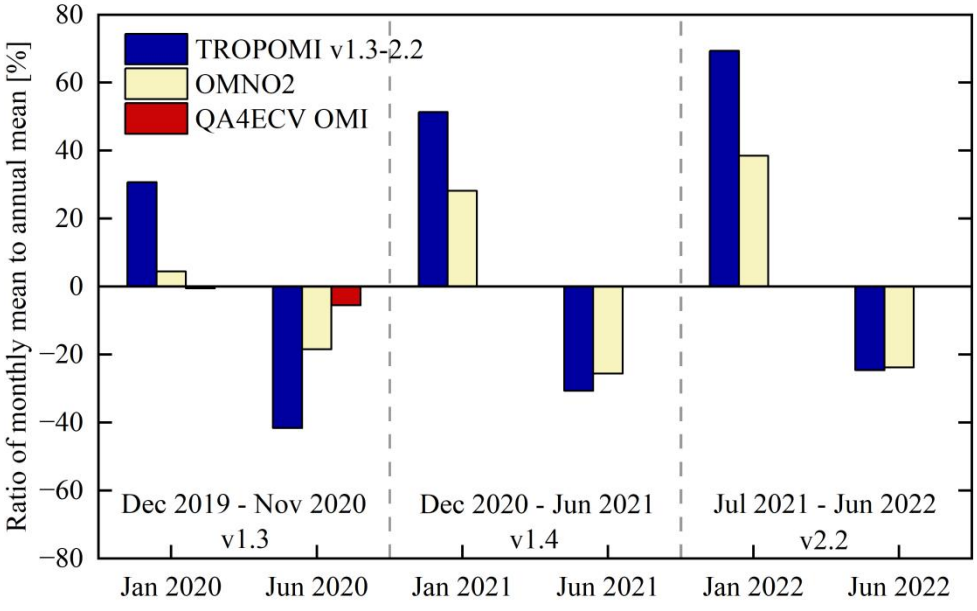

Figure 5. Ratios of the January and June mean tropospheric NO_2 VCD in each period (December 2019-November 2020, December 2020-June 2021, July 2021-June 2022) to the averaged tropospheric NO_2 VCD over the period retrieved from TROPOMI, OMNO2 and QA4ECV OMI observations over China.

Overall, TROPOMI data shows strongest seasonal variation of tropospheric NO_2 columns compared to OMNO2 data and QA4ECV OMI data. During all three periods, compared to the averages over the entire periods, the extents of the observed NO_2 changes in winter or summer month retrieved from TROPOMI exceed those retrieved from OMI (Fig. 5). Although QA4ECV OMI follows a more similar NO_2 retrieval algorithm to TROPOMI relative to OMNO2, the increase in winter and decrease in summer of NO_2 observed with QA4ECV OMI (−0.5 % and -5 %) are even smaller than those observed with OMNO2 (4 % and -18 %) over China. Taking

https://doi.org/10.5194/egusphere-2023-175
Preprint. Discussion started: 17 March 2023

this into account, and the strong seasonal variation of tropospheric NO_2 columns present in TROPOMI version 1.3-2.2 data, we conclude that the FRESCO (FRESCO-wide) cloud algorithm using in the NO_2 retrieval has a positive impact on the clear demonstration of seasonal variation of TROPOMI tropospheric NO_2.

We find that with the introduction of the FRESCO-wide algorithm in version 1.4 and the adjusted surface albedo in version 2.2, the ratio of the January mean NO_2 column to the averaged NO_2 column is increased by 21 % and 39 % in TROPOMI version 1.4 and 2.2 than in version 1.3 over China, respectively. But the ratio for June in version 1.4 and 2.2 is decreased by 11 and 17 % than in version 1.3. As a consequence, the changes in the TROPOMI NO_2 retrieval version 1.3-2.2 lead to form stronger (weaker) effect of tropospheric NO_2 seasonal variation in winter (summer). This can be explained by the seasonal variation of cloud pressure (Ri et al., 2022), which is provided more realistic by the FRESCO-wide cloud algorithm in TROPOMI version 1.4, for instance in the case of low clouds, as well as the adjusted surface albedo for cloud-free scenes in version 2.2, which can occur more commonly in winter than in summer. Since up to date the TROPOMI NO_2 version 2.4 data is available for only two months, its seasonal variation could be studied in future.

We also create the daily tropospheric NO_2 VCDs derived from TROPOMI, OMNO2 and QA4ECV OMI observations over the BTH, YRD and PRD region in China to compare (Fig. 6). As a result, the monthly means of tropospheric NO_2 VCDs between November 2019 to November 2020 over BTH region are 3.41 ± 0.65 (TROPOMI), 3.01 ± 0.78 (OMNO2) and 4.31 ± 2.24 (QA4ECV OMI) times higher than over China, respectively. Moreover, these higher trends reached a maximum of 4.37 (in January, TROPOMI), 4.16 (in January, OMNO2), 8.62 (in January, QA4ECV OMI), and a minimum of 1.94 (in September, TROPOMI), 1.62 (in August, OMNO2), 2.11 (in June, QA4ECV OMI). Similar trends exist over other regions with high pollution (e.g. YRD and PRD), as demonstrated by Fig. 6. Consequently, these selected pollution regions show more

https://doi.org/10.5194/egusphere-2023-175
Preprint. Discussion started: 17 March 2023

significant tropospheric NO_2 columns in winter due to anthropogenic emissions. Additionally, we calculate the differences between TROPOMI and QA4ECV OMI tropospheric NO_2 daily VCDs for each selected pollution region and each month from November 2019 to November 2020. We see that the ratio of the TROPOMI NO_2 VCD to the QA4ECV OMI NO_2 VCD was closest to 1 in summer months (e.g. 0.93 in July for BTH, 0.97 in July for YRD, 1.00 in July for PRD), and farthest to 1 in winter months (e.g. 0.55 in February for BTH, 0.71 in December for YRD, 0.66 in January for PRD). Therefore, compared to the QA4ECV OMI NO_2 retrieval, the FRESCO cloud algorithm using in the TROPOMI NO_2 retrieval has a strongly positive impact on the tropospheric NO_2 seasonal cycle, especially in high pollution regions in winter.

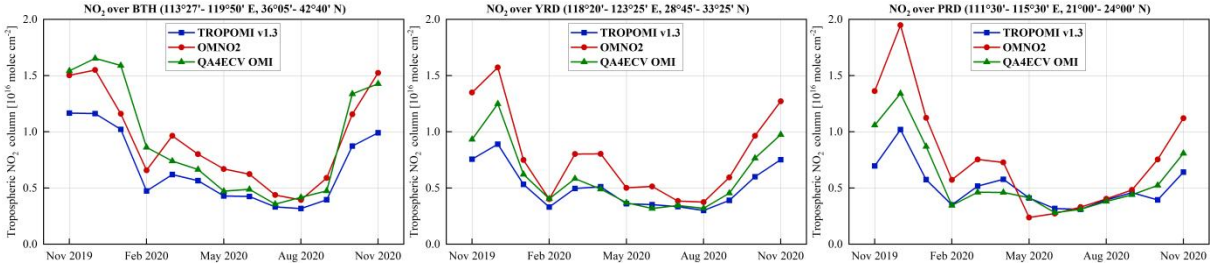

Figure 6. Time series of TROPOMI version 1.3, OMNO2 and QA4ECV OMI tropospheric NO_2 columns over the BTH, YRD, PRD region, which is typical of high NO_2 pollution conditions in China.

3.4 AMFs and NO_2 column biases

AMF uncertainties dominate overall satellite-derived NO_2 retrieval errors over polluted regions (Boersma et al., 2004; Lamsal et al., 2014; Lorente et al., 2017; Martin et al., 2002). For this analysis, we create TROPOMI tropospheric AMF daily data from January 2020 to August 2022 at a resolution of 7 x 7 km^2, to study its changes in the upgrades from version 1.3-2.4 over China (Fig. 7). As a result, the daily AMFs in version 1.4 are lower (of up to 32 %, on 9 February) than in version 1.3. We find that the AMF reduction from version 1.3-1.4, exhibits a

https://doi.org/10.5194/egusphere-2023-175
Preprint. Discussion started: 17 March 2023

winter maximum (0.30, 16 % for January and 0.33, 18 % for February) and summer minimum (0.06, 5 % for May and 0.07, 5 % for June). We conclude that this TROPOMI AMF reduction, range between about 5 % in summer and 20 % in winter, is mainly due to the implement of the FRESCO-wide algorithm in the operational NO_2 version 1.4. Furthermore, the difference of this reduction in different months is caused by the seasonal variation of cloud pressure, which is consistent with the seasonal reduction in TROPOMI tropospheric NO_2 VCDs from version 1.3 to 1.4, as described in Section 3.3. The TROPOMI tropospheric AMFs in version 1.3-2.4 from 2020 to 2022 over China is given (Table 2).

https://doi.org/10.5194/egusphere-2023-175
Preprint. Discussion started: 17 March 2023

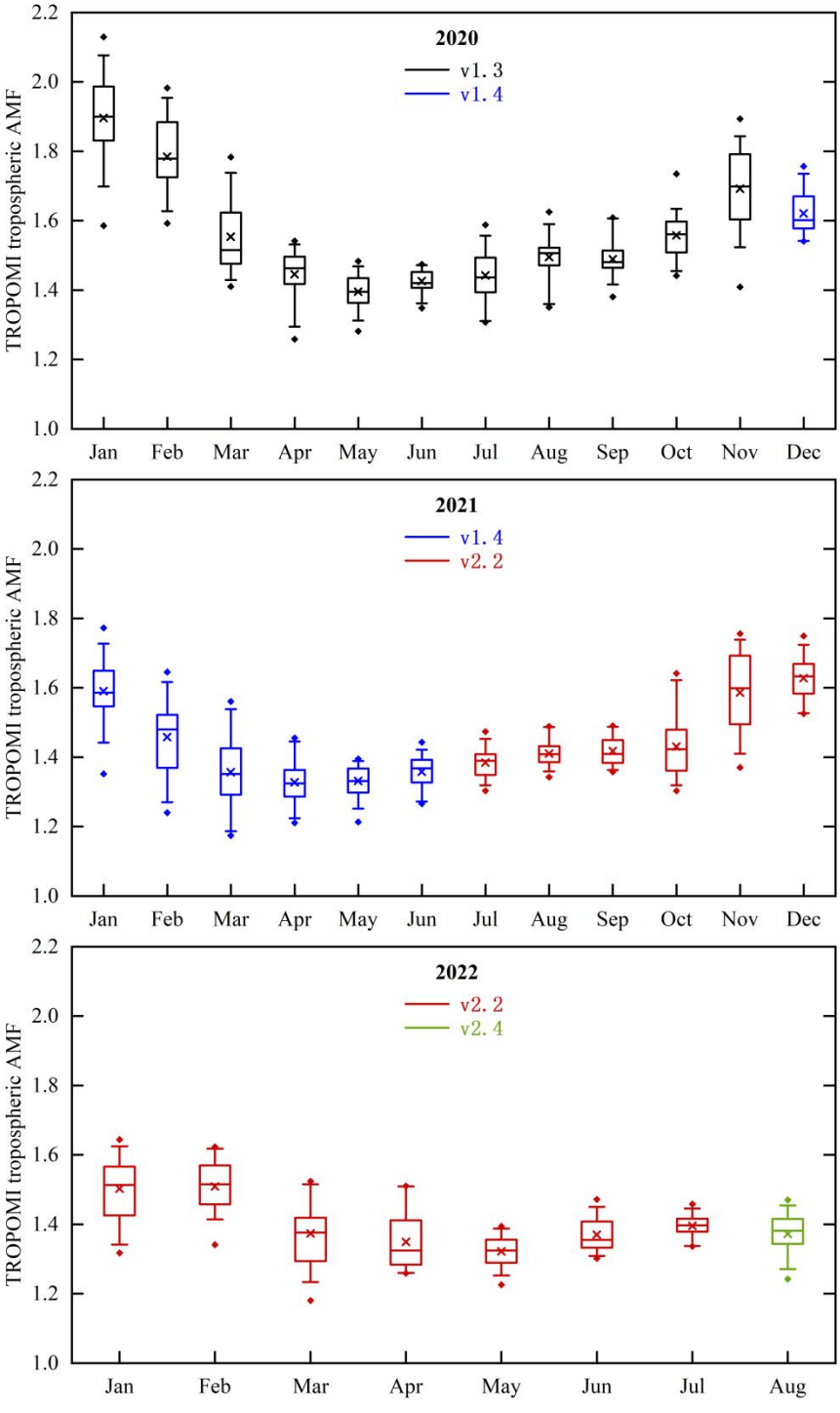

438

https://doi.org/10.5194/egusphere-2023-175
Preprint. Discussion started: 17 March 2023

Figure 7. Boxplots of TROPOMI tropospheric daily AMFs in version 1.3 (black), 1.4 (blue), 2.2 (red) and 2.4 (green) from 2020 to 2022 over China.

Table 2. TROPOMI tropospheric AMF data in version 1.3-2.4 from January 2020 to August 2022 over China.

Month	tropospheric AMF (v1.3)	tropospheric AMF v1.4-1.3 difference	tropospheric AMF v2.2-1.3 difference	tropospheric AMF v2.2-1.4 difference	tropospheric AMF v2.4-2.2 difference
Jan	1.89 ± 0.12	-0.30 ± 0.14	na	-0.09 ± 0.09	na
Feb	1.78 ± 0.11	-0.33 ± 0.12	na	0.05 ± 0.15	na
Mar	1.54 ± 0.13	-0.18 ± 0.14	na	0.02 ± 0.12	na
Apr	1.43 ± 0.10	-0.13 ± 0.10	na	0.03 ± 0.09	na
May	1.38 ± 0.08	-0.06 ± 0.09	na	0.00 ± 0.09	na
Jun	1.43 ± 0.03	-0.07 ± 0.05	na	0.01 ± 0.05	na
Jul	1.43 ± 0.09	na	-0.06 ± 0.06	na	na
Aug	1.50 ± 0.06	na	-0.08 ± 0.07	na	-0.04 ± 0.07
Sep	1.49 ± 0.05	na	-0.07 ± 0.06	na	na
Oct	1.56 ± 0.06	na	-0.13 ± 0.10	na	na
Nov	1.69 ± 0.12	na	-0.11 ± 0.12	na	na
Dec	na	na	na	0.01 ± 0.07	na

The difference of TROPOMI tropospheric AMF from version 1.4 to 2.2 is relatively minor as compared to that from version 1.3 to 1.4 (Fig. 7), range between a 5 % overestimation and a 3 % underestimation over China. This is in agreement with the larger difference of TROPOMI tropospheric NO_2 column from version 1.3 to 1.4

https://doi.org/10.5194/egusphere-2023-175
Preprint. Discussion started: 17 March 2023

relative to that from version 1.4 to 2.2, as described in Section 3.1, reflecting that although the adjusted surface albedo in version 2.2 could lead to significant decrease of tropospheric AMF, and subsequently increase of tropospheric NO_2 column for cloud-free scenes, but indeed, the extent of the change in tropospheric NO_2 column caused by it is generally smaller than that caused by the improvements of cloud pressure and cloud fraction in version 1.4 at the national scale. Additionally, we calculate the TROPOMI tropospheric AMF daily data in August of 2021 (version 2.2) and 2022 (version 2.4) over China, and find that the TROPOMI AMFs in version 2.4 using the DLER climatology are 0.04 ± 0.07 lower than in version 2.2.

We also compare the TROPOMI tropospheric AMF version 1.3 daily data to the QA4ECV OMI tropospheric AMF version 1.1 daily data from January to November 2020 over China. As a result, the TROPOMI AMFs are higher by 1.57 ± 0.96 times compared to the QA4ECV OMI AMFs, mainly due to the differences in their clouds retrievals using in the tropospheric AMF calculation. Moreover, we find that in all seasons, the TROPOMI AMFs are higher than the QA4ECV OMI AMFs by factors of 1.42 ± 0.13 in January, 0.87 ± 0.09 in April, of 0.64 ± 0.08 in July, and 0.72 ± 0.05 in October. This change of increment magnitude in different months is mainly due to the seasonal variation of the cloud pressure using in the TROPOMI NO_2 retrieval.

The biases of TROPOMI tropospheric AMFs in different versions presented above have a dominated impact on the biases of the TROPOMI tropospheric NO_2 columns retrieved under these version conditions. Thus, we calculate the differences of TROPOMI tropospheric AMF from version 1.3 to 1.4 to 2.2 over China. Then, we combine TROPOMI tropospheric NO_2 column data and the adjusted tropospheric AMFs by using the differences among the versions, to correct for the effect of the overestimation of the AMFs used in the previous NO_2 version retrievals. We take the TROPOMI tropospheric AMF version 2.2 data as reference, and calculate the daily ratios of the AMFs in previous versions and it in the same locations, then the AMFs in these previous versions are (at

https://doi.org/10.5194/egusphere-2023-175
Preprint. Discussion started: 17 March 2023

470 least partly) adjusted to avoid the effect of the overestimation. The TROPOMI tropospheric NO_2 columns in
471 these previous versions are thus (partly) corrected by combining the adjusted AMFs and the original observed
472 slant columns. The result is provided in Fig. 8, with increasing of tropospheric NO_2 column of up to 22 % as
473 compared to the TROPOMI data products.
474

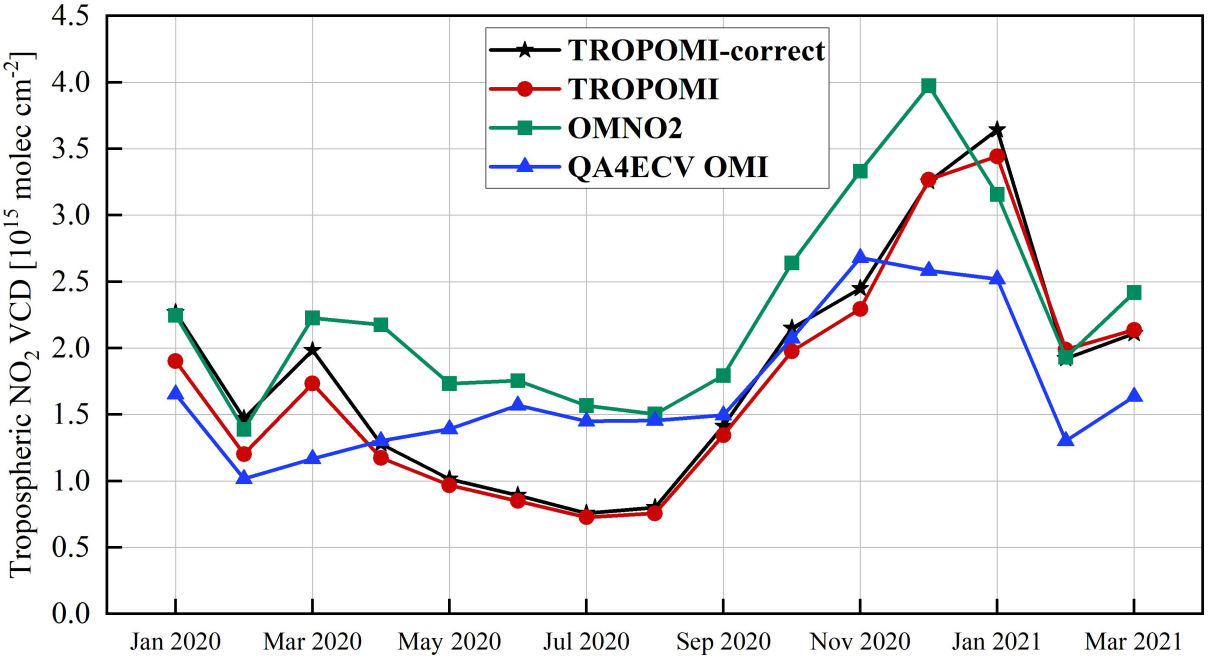

475

476 **Figure 8.** Time series of tropospheric NO_2 column monthly means retrieved from TROPOMI (red), TROPOMI
477 with corrected by AMF (black), OMNO2 (green) and QA4ECV OMI (blue) observations over China.
478

479 **3.5 NO_2 changes during lockdown**

480 China implemented nationwide restrictions to halt the spread of COVID-19 after the 2020 Spring Festival, such
481 as implementing strict travel restrictions and suspending factory productions. The nationwide lockdown in China

https://doi.org/10.5194/egusphere-2023-175
Preprint. Discussion started: 17 March 2023

due to the outbreak of COVID-19 caused large-scale and prolonged shutdowns in rural and urban areas, consequently, leading to a significant reduction of NO_2. In this section we use tropospheric NO_2 column data derived from TROPOMI, OMNO2 and QA4ECV OMI observations to evaluate their sensitivities to detect the NO_2 changes during the COVID-19 lockdown.

We first linearly interpolate the tropospheric NO_2 VCDs derived from TROPOMI, OMNO2 and QA4ECV OMI in February of 2019 and 2021, to create the expected tropospheric NO_2 VCDs in February 2020 over China. Then, we calculate the differences between the observed VCDs and the expected VCDs in February 2020 to demonstrate the NO_2 reduction during the COVID-19 lockdown (Fig. 9). As a result, the reduction during lockdown derived from TROPOMI (9.97×10^{14} molecules cm^{-2}) is significantly greater than from OMNO2 (5.89×10^{14} molecules cm^{-2}) and QA4ECV OMI (3.25×10^{14} molecules cm^{-2}). Moreover, the extent of this NO_2 reduction is larger over high pollution regions (e.g. for the BTH region, 3.75×10^{15} molecules cm^{-2} in TROPOMI, 2.75×10^{15} molecules cm^{-2} in OMNO2 and 5.85×10^{14} molecules cm^{-2} in QA4ECV OMI), due to the stronger impact of lockdown on these regions with large numbers of industrial facilities and heavy traffic flows. It is worth noting that the TROPOMI NO_2 VCD data in February 2019 using to create the expected NO_2 VCD during lockdown is retrieved in version 1.3, as well as the observed NO_2 VCD data in February 2020 using to compare. But the NO_2 VCD data in February 2021, another data source for creating the expected NO_2 VCD, is retrieved in version 1.4. Thus, we use the adjusted TROPOMI tropospheric AMFs as described in Section 3.4, to correct the TROPOMI tropospheric NO_2 VCDs in February of 2019 and 2020 with a low bias. We find that the reduction of tropospheric NO_2 column during lockdown using the adjusted AMFs is 6.66×10^{14} molecules cm^{-2} over China, reflecting that an overestimation of NO_2 column reduction during lockdown could be caused by using TROPOMI data before and after the activation of version 1.4.

https://doi.org/10.5194/egusphere-2023-175
Preprint. Discussion started: 17 March 2023

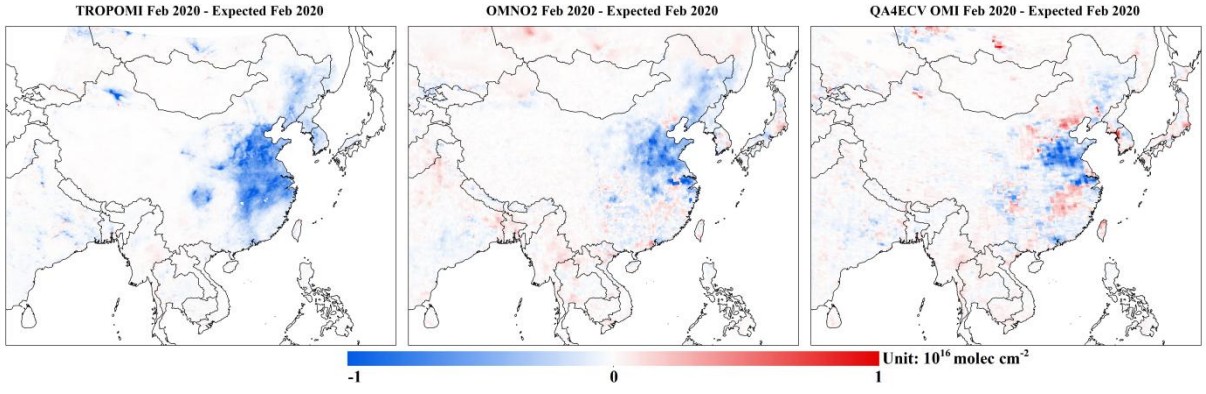

505

506 **Figure 9.** Differences between the observed and the expected tropospheric NO_2 column derived from TROPOMI
507 (left panel), OMNO2 (center panel) and QA4ECV OMI (right panel) in February 2020.

508

509 **4 Conclusion**

510 In this work, tropospheric NO_2 columns of the TROPOMI version 1.3-2.4 data product are validated using OMI-
511 derived OMNO2 data and QA4ECV data. The tropospheric column, spatial-temporal distribution, seasonal
512 variation of the TROPOMI NO_2 data in the different versions are presented and compared to the OMNO2 and
513 QA4ECV OMI NO_2 observations over China. In addition, the changes of the TROPOMI AMFs under the
514 different NO_2 retrieval version conditions are measured. The major conclusions are summarized as follows.

515

516 (1) The tropospheric NO_2 columns derived from TROPOMI version 1.3 data are lower than those derived from
517 OMNO2 data (54 %) and QA4ECV OMI data (50 %) over China, which mainly due to the overestimation of
518 cloud pressure retrieved by the FRESCO cloud retrieval algorithm, and subsequently the overestimation of the
519 AMF for scenes with small cloud fractions. As a consequence, a significant increase by 38 % of tropospheric
520 NO_2 columns, derived with the version 1.4 improved FRESCO-wide cloud retrieval, was identified as compared

https://doi.org/10.5194/egusphere-2023-175
Preprint. Discussion started: 17 March 2023

with the previous version. Moreover, TROPOMI tropospheric NO_2 column in version 2.2 is 14 % higher than in version 1.4, due to the adjusted surface albedo for cloud-free scenes.

(2) The upgrade to the current TROPOMI NO_2 version 2.4 with the DLER surface albedo led to a significant increase by 3.44 x 10^{14} molecules cm^{-2} of tropospheric NO_2 columns over vegetation, as compared with the previous version, due to the strong effect of the DLER over vegetation in the near infrared. Moreover, the results for tropospheric NO_2 seasonal variation by comparison of TROPOMI NO_2 version 1.3-2.2 data with OMNO2 data and QA4ECV OMI data are provided. TROPOMI data shows strongest tropospheric NO_2 seasonal variation compared to the other data. Additionally, the changes in the TROPOMI NO_2 version 1.3-2.2 retrievals lead to enhance the seasonal effect of tropospheric NO_2, due to the seasonal variation of cloud pressure which is provided more realistic by the FRESCO-wide cloud algorithm in version 1.4 and the adjusted surface albedo for cloud-free scenes in version 2.2.

(3) TROPOMI AMF in version 1.4 is lower by 32 % than in version 1.3, mainly due to the implementation of the FRESCO-wide algorithm. The difference of TROPOMI AMF from version 1.4 to 2.2 is relatively minor, range between a 5 % overestimation and a 3 % underestimation due to the adjusted surface albedo. The TROPOMI AMF in version 2.4 using the DLER climatology is 3 % lower than in version 2.2. Overall, the TROPOMI AMF in version 1.3-2.4 over China is given, and based on it, the effects of the underestimation of TROPOMI tropospheric NO_2 column in the previous version retrievals are (at least partly) addressed. In addition, the reduction of NO_2 column during COVID-19 lockdown using the adjusted TROPOMI AMF is presented, and a 33 % overestimation of NO_2 column reduction during lockdown is measured as compared to the TROPOMI NO_2 data products, due to using TROPOMI data before and after the activation of the NO_2 version 1.4.

https://doi.org/10.5194/egusphere-2023-175
Preprint. Discussion started: 17 March 2023

Data availability.

TROPOMI data are obtained from (https://disc.gsfc.nasa.gov/datasets); OMNO2 data are obtained from (https://aura.gesdisc.eosdis.nasa.gov/data); QA4ECV OMI data are obtained from (http://www.qa4ecv.eu/ecvs).

Author contributions.

Jianbin Gu: Conceptualization, Methodology, Writing - original draft. **Jinhua Tao:** Data curation. **Xiaoxia Liang and Shipeng Song:** Validation. **Yanfang Tian and Liangfu Chen:** Writing - review & editing.

Declaration of competing interest.

The authors declare that they have no known competing financial interests or personal relationships that could have appeared to influence the work reported in this paper.

Acknowledgements.

We gratefully acknowledge TROPOMI, OMI and QA4ECV science teams for making data publicly available.

Funding.

This research did not receive any specific grant from funding agencies in the public, commercial, or not-for-profit sectors.

References

https://doi.org/10.5194/egusphere-2023-175
Preprint. Discussion started: 17 March 2023

564 van der A, R. J., Peters, D. H. M. U., Eskes, H., Boersma, K. F., Van Roozendael, M., De Smedt, I. and Kelder,
565 H. M.: Detection of the trend and seasonal variation in tropospheric NO_2 over China, J. Geophys. Res. Atmos.,
566 111(12), 1–10, doi:10.1029/2005JD006594, 2006.
567 van der A, R. J., de Laat, A. T. J., Ding, J. and Eskes, H. J.: Connecting the dots: NOx emissions along a West
568 Siberian natural gas pipeline, npj Clim. Atmos. Sci., 3(1), 1–7, doi:10.1038/s41612-020-0119-z, 2020.
569 Bauwens, M., Compernolle, S., Stavrakou, T., Müller, J. F., van Gent, J., Eskes, H., Levelt, P. F., van der A, R.,
570 Veefkind, J. P., Vlietinck, J., Yu, H. and Zehner, C.: Impact of Coronavirus Outbreak on NO_2 Pollution Assessed
571 Using TROPOMI and OMI Observations, Geophys. Res. Lett., 47(11), 1–9, doi:10.1029/2020GL087978, 2020.
572 Biswal, A., Singh, V., Singh, S., Kesarkar, A. P., Ravindra, K., Sokhi, R. S., Chipperfield, M. P., Dhomse, S. S.,
573 Pope, R. J., Singh, T. and Mor, S.: COVID-19 lockdown-induced changes in NO_2 levels across India observed
574 by multi-satellite and surface observations, Atmos. Chem. Phys., 21(6), 5235–5251, doi:10.5194/acp-21-5235-
575 2021, 2021.
576 Boersma, K. F., Eskes, H. J. and Brinksma, E. J.: Error analysis for tropospheric NO_2 retrieval from space, J.
577 Geophys. Res. Atmos., 109(4), doi:10.1029/2003jd003962, 2004.
578 Boersma, K. F., Eskes, H. J., Veefkind, J. P., Brinksma, E. J., Van Der A, R. J., Sneep, M., Van Den Oord, G. H.
579 J., Levelt, P. F., Stammes, P., Gleason, J. F. and Bucsela, E. J.: Near-real time retrieval of tropospheric NO_2 from
580 OMI, Atmos. Chem. Phys., 7(8), 2103–2118, doi:10.5194/acp-7-2103-2007, 2007.
581 Boersma, K. F., Eskes, H. J., Richter, A., De Smedt, I., Lorente, A., Beirle, S., Van Geffen, J. H. G. M., Zara, M.,
582 Peters, E., Van Roozendael, M., Wagner, T., Maasakkers, J. D., Van Der A, R. J., Nightingale, J., De Rudder, A.,
583 Irie, H., Pinardi, G., Lambert, J. C. and Compernolle, S. C.: Improving algorithms and uncertainty estimates for
584 satellite NO_2 retrievals: Results from the quality assurance for the essential climate variables (QA4ECV) project,
585 Atmos. Meas. Tech., 11(12), 6651–6678, doi:10.5194/amt-11-6651-2018, 2018.

https://doi.org/10.5194/egusphere-2023-175
Preprint. Discussion started: 17 March 2023

586 Bucsela, E. J., Krotkov, N. A., Celarier, E. A., Lamsal, L. N., Swartz, W. H., Bhartia, P. K., Boersma, K. F.,
587 Veefkind, J. P., Gleason, J. F. and Pickering, K. E.: A new stratospheric and tropospheric NO_2 retrieval
588 algorithm for nadir-viewing satellite instruments: Applications to OMI, Atmos. Meas. Tech., 6(10), 2607–2626,
589 doi:10.5194/amt-6-2607-2013, 2013.
590 Celarier, E. A., Brinksma, E. J., Gleason, J. F., Veerkind, J. P., Cede, A., Herman, J. R., Ionov, D., Goutail, F.,
591 Pommereau, J. P., Lambert, J. C., Van Roozendael, M., Pinardi, G., Wittrock, F., Schönhardt, A., Richter, A.,
592 Ibrahim, O. W., Wagner, T., Bojkov, B., Mount, G., Spinei, E., Chen, C. M., Pongetti, T. J., Sander, S. P.,
593 Bucsela, E. J., Wenig, M. O., Swart, D. P. J., Volten, H., Kroon, M. and Levelt, P. F.: Validation of ozone
594 monitoring instrument nitrogen dioxide columns, J. Geophys. Res. Atmos., 113(15), 1–23,
595 doi:10.1029/2007JD008908, 2008.
596 Compernolle, S., Verhoelst, T., Pinardi, G., Granville, J., Hubert, D., Keppens, A., Niemeijer, S., Rino, B., Bais,
597 A., Beirle, S., Boersma, F., Burrows, J. P., De Smedt, I., Eskes, H., Goutail, F., Hendrick, F., Lorente, A.,
598 Pazmino, A., Piters, A., Peters, E., Pommereau, J. P., Remmers, J., Richter, A., Van Geffen, J., Van Roozendael,
599 M., Wagner, T. and Lambert, J. C.: Validation of Aura-OMI QA4ECV NO_2 climate data records with ground-
600 based DOAS networks: The role of measurement and comparison uncertainties, Atmos. Chem. Phys., 20(13),
601 8017–8045, doi:10.5194/acp-20-8017-2020, 2020.
602 Cooper, M. J., Martin, R. V., Hammer, M. S., Levelt, P. F., Veefkind, P., Lamsal, L. N., Krotkov, N. A., Brook,
603 J. R. and McLinden, C. A.: Global fine-scale changes in ambient NO_2 during COVID-19 lockdowns, Nature,
604 601(7893), 380–387, doi:10.1038/s41586-021-04229-0, 2022.
605 Curier, R. L., Kranenburg, R., Segers, A. J. S., Timmermans, R. M. A. and Schaap, M.: Synergistic use of OMI
606 NO_2 tropospheric columns and LOTOS-EUROS to evaluate the NOx emission trends across Europe, Remote
607 Sens. Environ., 149(2), 58–69, doi:10.1016/j.rse.2014.03.032, 2014.

https://doi.org/10.5194/egusphere-2023-175
Preprint. Discussion started: 17 March 2023

608 Dimitropoulou, E., Hendrick, F., Pinardi, G., Friedrich, M. M., Merlaud, A., Tack, F., De Longueville, H., Fayt,
609 C., Hermans, C., Laffineur, Q., Fierens, F. and Van Roozendael, M.: Validation of TROPOMI tropospheric NO_2
610 columns using dual-scan multi-axis differential optical absorption spectroscopy (MAX-DOAS) measurements in
611 Uccle, Brussels, Atmos. Meas. Tech., 13(10), 5165–5191, doi:10.5194/amt-13-5165-2020, 2020.
612 Ding, J., van der A, R. J., Eskes, H. J., Mijling, B., Stavrakou, T., van Geffen, J. H. G. M. and Veefkind, J. P.:
613 NOx Emissions Reduction and Rebound in China Due to the COVID-19 Crisis, Geophys. Res. Lett., 47(19), 1–9,
614 doi:10.1029/2020GL089912, 2020.
615 Fasnacht, Z., Vasilkov, A., Haffner, D., Qin, W., Joiner, J., Krotkov, N., Sayer, A. M. and Spurr, R.: A
616 geometry-dependent surface Lambertian-equivalent reflectivity product for UV-Vis retrievals - Part 2:
617 Evaluation over open ocean, Atmos. Meas. Tech., 12(12), 6749–6769, doi:10.5194/amt-12-6749-2019, 2019.
618 Van Geffen, J., Folkert Boersma, K., Eskes, H., Sneep, M., Ter Linden, M., Zara, M. and Pepijn Veefkind, J.:
619 S5P TROPOMI NO_2 slant column retrieval: Method, stability, uncertainties and comparisons with OMI, Atmos.
620 Meas. Tech., 13(3), 1315–1335, doi:10.5194/amt-13-1315-2020, 2020.
621 Van Geffen, J., Eskes, H., Compernolle, S., Pinardi, G., Verhoelst, T., Lambert, J. C., Sneep, M., Linden, M. Ter,
622 Ludewig, A., Folkert Boersma, K. and Pepijn Veefkind, J.: Sentinel-5P TROPOMI NO_2 retrieval: impact of
623 version v2.2 improvements and comparisons with OMI and ground-based data, Atmos. Meas. Tech., 15(7),
624 2037–2060, doi:10.5194/amt-15-2037-2022, 2022.
625 Goldberg, D. L., Lamsal, L. N., Loughner, C. P., Swartz, W. H., Lu, Z. and Streets, D. G.: A high-resolution and
626 observationally constrained OMI NO_2 satellite retrieval, Atmos. Chem. Phys., 17(18), 11403–11421,
627 doi:10.5194/acp-17-11403-2017, 2017.
628 Griffin, D., Zhao, X., McLinden, C. A., Boersma, F., Bourassa, A., Dammers, E., Degenstein, D., Eskes, H.,
629 Fehr, L., Fioletov, V., Hayden, K., Kharol, S. K., Li, S. M., Makar, P., Martin, R. V., Mihele, C., Mittermeier, R.
630 L., Krotkov, N., Sneep, M., Lamsal, L. N., Linden, M. ter, Geffen, J. van, Veefkind, P. and Wolde, M.: High-

https://doi.org/10.5194/egusphere-2023-175
Preprint. Discussion started: 17 March 2023

631 Resolution Mapping of Nitrogen Dioxide With TROPOMI: First Results and Validation Over the Canadian Oil
632 Sands, Geophys. Res. Lett., 46(2), 1049–1060, doi:10.1029/2018GL081095, 2019.
633 Gu, J., Chen, L., Yu, C., Li, S., Tao, J., Fan, M., Xiong, X., Wang, Z., Shang, H. and Su, L.: Ground-level NO_2
634 concentrations over China inferred from the satellite OMI and CMAQ model simulations, Remote Sens., 9(6),
635 doi:10.3390/rs9060519, 2017.
636 Kim, M., Brunner, D. and Kuhlmann, G.: Importance of satellite observations for high-resolution mapping of
637 near-surface NO_2 by machine learning, Remote Sens. Environ., 264(February), 112573,
638 doi:10.1016/j.rse.2021.112573, 2021.
639 Kleipool, Q. L., Dobber, M. R., de Haan, J. F. and Levelt, P. F.: Earth surface reflectance climatology from 3
640 years of OMI data, J. Geophys. Res. Atmos., 113(18), 1–22, doi:10.1029/2008JD010290, 2008.
641 Krotkov, N. A., Lamsal, L. N., Celarier, E. A., Swartz, W. H., Marchenko, S. V., Bucsela, E. J., Chan, K. L.,
642 Wenig, M. and Zara, M.: The version 3 OMI NO_2 standard product, Atmos. Meas. Tech., 10(9), 3133–3149,
643 doi:10.5194/amt-10-3133-2017, 2017.
644 Lamsal, L. N., Krotkov, N. A., Celarier, E. A., Swartz, W. H., Pickering, K. E., Bucsela, E. J., Gleason, J. F.,
645 Martin, R. V., Philip, S., Irie, H., Cede, A., Herman, J., Weinheimer, A., Szykman, J. J. and Knepp, T. N.:
646 Evaluation of OMI operational standard NO_2 column retrievals using in situ and surface-based NO_2 observations,
647 Atmos. Chem. Phys., 14(21), 11587–11609, doi:10.5194/acp-14-11587-2014, 2014.
648 Levelt, P. F., Van Den Oord, G. H. J., Dobber, M. R., Mälkki, A., Visser, H., De Vries, J., Stammes, P., Lundell,
649 J. O. V. and Saari, H.: The ozone monitoring instrument, IEEE Trans. Geosci. Remote Sens., 44(5), 1093–1100,
650 doi:10.1109/TGRS.2006.872333, 2006.
651 Levelt, P. F., Joiner, J., Tamminen, J., Veefkind, J. P., Bhartia, P. K., Zweers, D. C. S., Duncan, B. N., Streets, D.
652 G., Eskes, H., Van Der, R. A., McLinden, C., Fioletov, V., Carn, S., De Laat, J., Deland, M., Marchenko, S.,
653 McPeters, R., Ziemke, J., Fu, D., Liu, X., Pickering, K., Apituley, A., Abad, G. G., Arola, A., Boersma, F.,

https://doi.org/10.5194/egusphere-2023-175
Preprint. Discussion started: 17 March 2023

Miller, C. C., Chance, K., De Graaf, M., Hakkarainen, J., Hassinen, S., Ialongo, I., Kleipool, Q., Krotkov, N., Li, C., Lamsal, L., Newman, P., Nowlan, C., Suleiman, R., Tilstra, L. G., Torres, O., Wang, H. and Wargan, K.: The Ozone Monitoring Instrument: Overview of 14 years in space, Atmos. Chem. Phys., 18(8), 5699–5745, doi:10.5194/acp-18-5699-2018, 2018.

Liu, F., Beirle, S., Zhang, Q., van der A, R., Zheng, B., Tong, D. and He, K.: NOx emission trends over Chinese cities estimated from OMI observations during 2005 to 2015, Atmos. Chem. Phys. Discuss., (2), 1–21, doi:10.5194/acp-2017-369, 2017a.

Liu, L., Zhang, X., Xu, W., Liu, X., Lu, X., Chen, D., Zhang, X., Wang, S. and Zhang, W.: Estimation of monthly bulk nitrate deposition in China based on satellite NO_2 measurement by the Ozone Monitoring Instrument, Remote Sens. Environ., 199, 93–106, doi:10.1016/j.rse.2017.07.005, 2017b.

Liu, S., Valks, P., Pinardi, G., Xu, J., Chan, K. L., Argyrouli, A., Lutz, R., Beirle, S., Khorsandi, E., Baier, F., Huijnen, V., Bais, A., Donner, S., Dörner, S., Gratsea, M., Hendrick, F., Karagkiozidis, D., Lange, K., Piters, A. J. M., Remmers, J., Richter, A., Van Roozendael, M., Wagner, T., Wenig, M. and Loyola, D. G.: An improved TROPOMI tropospheric NO_2 research product over Europe, Atmos. Meas. Tech., 14(11), 7297–7327, doi:10.5194/amt-14-7297-2021, 2021.

Lorente, A., Folkert Boersma, K., Yu, H., Dörner, S., Hilboll, A., Richter, A., Liu, M., Lamsal, L. N., Barkley, M., De Smedt, I., Van Roozendael, M., Wang, Y., Wagner, T., Beirle, S., Lin, J. T., Krotkov, N., Stammes, P., Wang, P., Eskes, H. J. and Krol, M.: Structural uncertainty in air mass factor calculation for NO_2 and HCHO satellite retrievals, Atmos. Meas. Tech., 10(3), 759–782, doi:10.5194/amt-10-759-2017, 2017.

Martin, R. V., Chance, K., Jacob, D. J., Kurosu, T. P., Spurr, R. J. D., Bucsela, E., Gleason, J. F., Palmer, P. I., Bey, I., Fiore, A. M., Li, Q., Yantosca, R. M. and Koelemeijer, R. B. A.: An improved retrieval of tropospheric nitrogen dioxide from GOME, J. Geophys. Res. D Atmos., 107(20), doi:10.1029/2001JD001027, 2002.

https://doi.org/10.5194/egusphere-2023-175
Preprint. Discussion started: 17 March 2023

Marchenko, S., Krotkov, N. A., Lamsal, L. N., Celarier, E. A., Swartz, W. H. and Bucsela, E. J.: Revising the slant column density retrieval of nitrogen dioxide observed by the ozone monitoring instrument, J. Geophys. Res., 120(11), 5670–5692, doi:10.1002/2014JD022913, 2015.

Meng, K., Xu, X., Cheng, X., Xu, X., Qu, X., Zhu, W., Ma, C., Yang, Y. and Zhao, Y.: Spatio-temporal variations in SO_2 and NO_2 emissions caused by heating over the Beijing-Tianjin-Hebei Region constrained by an adaptive nudging method with OMI data, Sci. Total Environ., 642(2), 543–552, doi:10.1016/j.scitotenv.2018.06.021, 2018.

Nowlan, C. R., Martin, R. V., Philip, S., Lamsal, L. N., Krotkov, N. A., Marais, E. A., Wang, S. and Zhang, Q.: Global dry deposition of nitrogen dioxide and sulfur dioxide inferred from space-based measurements, Global Biogeochem. Cycles, 28(10), 1025–1043, doi:10.1002/2014GB004805, 2014.

Park, H., Jeong, S., Park, H., Labzovskii, L. D. and Bowman, K. W.: An assessment of emission characteristics of Northern Hemisphere cities using spaceborne observations of CO_2, CO, and NO_2, Remote Sens. Environ., 254(March 2020), 112246, doi:10.1016/j.rse.2020.112246, 2021.

Ri, X., Tana, G., Shi, C., Nakajima, T. Y., Shi, J. and Zhao, J.: Cloud , Atmospheric Radiation and Renewal Energy Property Product From Himawari-8 / AHI : Algorithm Development and Preliminary Validation, , 60, doi:10.1109/TGRS.2022.3172228, 2022.

Riess, T. C. V. W., Boersma, K. F., Van Vliet, J., Peters, W., Sneep, M., Eskes, H. and Van Geffen, J.: Improved monitoring of shipping NO_2 with TROPOMI: Decreasing NOx emissions in European seas during the COVID-19 pandemic, Atmos. Meas. Tech., 15(5), 1415–1438, doi:10.5194/amt-15-1415-2022, 2022.

Schneider, P., Lahoz, W. A. and Van Der A, R.: Recent satellite-based trends of tropospheric nitrogen dioxide over large urban agglomerations worldwide, Atmos. Chem. Phys., 15(3), 1205–1220, doi:10.5194/acp-15-1205-2015, 2015.

https://doi.org/10.5194/egusphere-2023-175
Preprint. Discussion started: 17 March 2023

De Smedt, I., Theys, N., Yu, H., Danckaert, T., Lerot, C., Compernolle, S., Van Roozendael, M., Richter, A., Hilboll, A., Peters, E., Pedergnana, M., Loyola, D., Beirle, S., Wagner, T., Eskes, H., Van Geffen, J., Folkert Boersma, K. and Veefkind, P.: Algorithm theoretical baseline for formaldehyde retrievals from S5P TROPOMI and from the QA4ECV project, Atmos. Meas. Tech., 11(4), 2395–2426, doi:10.5194/amt-11-2395-2018, 2018.

Tilstra, L. G., Tuinder, O. N. E., Wang, P. and Stammes, P.: Surface reflectivity climatologies from UV to NIR determined from Earth observations by GOME-2 and SCIAMACHY, J. Geophys. Res., 122(7), 4084–4111, doi:10.1002/2016JD025940, 2017.

Vasilkov, A., Yang, E. S., Marchenko, S., Qin, W., Lamsal, L., Joiner, J., Krotkov, N., Haffner, D., Bhartia, P. K. and Spurr, R.: A cloud algorithm based on the O2-O2 477 nm absorption band featuring an advanced spectral fitting method and the use of surface geometry-dependent Lambertian-equivalent reflectivity, Atmos. Meas. Tech., 11(7), 4093–4107, doi:10.5194/amt-11-4093-2018, 2018.

Veefkind, J. P., Aben, I., McMullan, K., Förster, H., de Vries, J., Otter, G., Claas, J., Eskes, H. J., de Haan, J. F., Kleipool, Q., van Weele, M., Hasekamp, O., Hoogeveen, R., Landgraf, J., Snel, R., Tol, P., Ingmann, P., Voors, R., Kruizinga, B., Vink, R., Visser, H. and Levelt, P. F.: TROPOMI on the ESA Sentinel-5 Precursor: A GMES mission for global observations of the atmospheric composition for climate, air quality and ozone layer applications, Remote Sens. Environ., 120(2012), 70–83, doi:10.1016/j.rse.2011.09.027, 2012.

Wang, C., Wang, T., Wang, P. and Rakitin, V.: Comparison and validation of TROPOMI and OMI NO_2 observations over China, Atmosphere (Basel)., 11(6), doi:10.3390/atmos11060636, 2020.

Williams, J. E., Folkert Boersma, K., Le Sager, P. and Verstraeten, W. W.: The high-resolution version of TM5-MP for optimized satellite retrievals: Description and validation, Geosci. Model Dev., 10(2), 721–750, doi:10.5194/gmd-10-721-2017, 2017.

Zara, M., Boersma, K. F., De Smedt, I., Richter, A., Peters, E., Van Geffen, J. H. G. M., Beirle, S., Wagner, T., Van Roozendael, M., Marchenko, S., Lamsal, L. N. and Eskes, H. J.: Improved slant column density retrieval of

https://doi.org/10.5194/egusphere-2023-175
Preprint. Discussion started: 17 March 2023

721 nitrogen dioxide and formaldehyde for OMI and GOME-2A from QA4ECV: Intercomparison, uncertainty
722 characterisation, and trends, Atmos. Meas. Tech., 11(7), 4033–4058, doi:10.5194/amt-11-4033-2018, 2018.
723 Zhang, Q., Boersma, K. F., Zhao, B., Eskes, H., Chen, C., Zheng, H. and Zhang, X.: Quantifying daily NOx and
724 CO_2 emissions from Wuhan using satellite observations from TROPOMI and OCO-2 , Atmos. Chem. Phys.,
725 23(1), 551–563, doi:10.5194/acp-23-551-2023, 2023.
726 Zhao, X., Griffin, D., Fioletov, V., McLinden, C., Cede, A., Tiefengraber, M., Müller, M., Bognar, K., Strong,
727 K., Boersma, F., Eskes, H., Davies, J., Ogyu, A. and Chi Lee, S.: Assessment of the quality of tropomi high-
728 spatial-resolution NO_2 data products in the greater toronto area, Atmos. Meas. Tech., 13(4), 2131–2159,
729 doi:10.5194/amt-13-2131-2020, 2020.
730